

## Determination of High Strain-Rate Material Properties from Explosive Loading of Frames

Y. Kivity, D. Peretz

*Rafael Ballistics Center, P.O. Box 2250, Haifa, Israel*

### Abstract

We propose a combined experimental-computational procedure for determining the plastic behavior of ductile materials at high rates of strain. The experimental set-up consists of loading a structure impulsively using a thin layer of explosive (Deta Sheet). The structure is loaded either by direct contact with the explosive, or by impacting an explosively - accelerated projectile. The permanent deformations of the structure are measured and compared with computer code predictions to determine the constants in the assumed constitutive relations.

### 1. Introduction

Assessment of the vulnerability of a reactor system to a hypothetical extreme load often requires knowledge of the dynamic mechanical properties of ductile materials. In many cases this information is not available for the high strain-rates ( $10^3$ /sec) resulting from typical extreme loads.

In this paper we propose a combined experimental-computational procedure for characterizing the viscoplastic behavior of strain-rate sensitive metals. In this procedure, the permanent deflections of impulsively loaded structures are measured. In parallel, theoretical predictions of the deformations are obtained, assuming a given dependence between the yield strength and the strain rate. The parameters in the relation between yield stress and strain-rate are fitted by comparing the theoretical and measured deflections. This procedure can be expected to yield only gross quantitative results, but it often suffices for the desired vulnerability assessment studies.

Two materials were considered in this paper: mild steel and 6061T6 Aluminum. We assumed the following relations for mild steel<sup>[1]</sup> and Aluminum<sup>[2]</sup>, respectively

$$\frac{Y}{Y_0} = 1 + (d/d_0)^{1/n} \quad (1)$$

$$\frac{Y}{Y_0} = 1 + b \log d/d_0 \quad (2)$$

Where  $Y$  is the uniaxial yield stress,  $d$  is the strain-rate and  $n$ ,  $d_0$  and  $b$  are material parameters.  $Y_0$  is the static yield stress.

Two configurations were tested, and will be described in the experimental section. The considerations in their choice were: (a) simplicity in manufacture, (b) accuracy in determining the impulsive load, and (c) clarity in the computational modeling. The latter consideration is important since the method relies on faithful modeling of the problem (and boundary conditions) in determining the constants in the constitutive law.

## 2. Experimental Set-up

The first configuration involves impacting a water-filled cylinder by an explosively accelerated disc. (Fig. 1). The disc acceleration system consists of a thin layer of explosive (DuPont Deta Sheet) sandwiched between the projectile disc, and a backup plate. The Deta Sheet is ignited at its center, to achieve axisymmetric acceleration. The disc velocity is controlled by the thicknesses of the explosive and the backup plate. The velocity resulting from each system was determined in separate experiments by measuring the flight time of the disc to various distances using a contact probe.

The disc acceleration system and the cylinder were aligned to ensure axisymmetric deformation. The water was poured through two openings in the rear end, which were closed after filling. Special care was taken to prevent air bubbles from being trapped.

A set of coordinates (circles 10mm apart and six equally spaced generators) were marked on the surface of the cylinder by very fine grooves. The permanent displacements of the coordinate points were measured after the test.

In the second configuration, a frame is loaded by placing the explosive in direct contact with it. To ensure clamping conditions, the frame was fabricated by milling of a solid plate. (Fig. 2a). The frame is held between two heavy plates to prevent the detonation products from moving in a directions normal to the plane of the frame, and thus simulate plane 2D flow of the detonation products. The impulse imparted to the frame section in contact with the explosive is determined by measuring the velocity of a bar accelerated in identical conditions (Fig. 2b).

## 3. Computational Modeling

Modeling of the experiments was carried out with the 2D code DISCO. This code couples the motions of a fluid and a structure in contact with it, with full sliding at the interface. Both the fluid and the structure zones are described in Lagrange coordinates. The fluid zone is a 2D continuum, while the structure is described by thin shell theory and is therefore represented as a curved line in 2D space. The numerical schemes are given in detail in <sup>[3]</sup>. The code was validated by participation in the APRICOT<sup>[4]</sup> programme, where its predictions for test problems compared favorably with those obtained from well known codes.

In both experiments, conditions of impulsive loading were assumed, i.e. a part of the structure was given an initial velocity that corresponds to the impulsive load, and its motion was then followed until the kinetic energy was dissipated into plastic energy. The dynamic relaxation method<sup>[5]</sup> was employed to damp elastic vibration at the end of the plastic phase of the motion.

The computer simulation requires the definition of the equation of state for the fluid and a constitutive relation for the thin shell. The behavior of water in compression was modeled by the following equation of state (Seeger and Polachek<sup>[6]</sup>):

$$e = \frac{(p+a)v}{\gamma-1}$$

Where  $e$  is the specific internal energy,  $p$  is the pressure and  $v$  is the specific volume, and  $a$  and  $\gamma$  are parameters with the values:

$$a=0.300\text{GPa} \quad , \quad \gamma=7.15$$

It is assumed that water can support no tension, and the pressure was restricted to  $p>0$ .

For the cylinders and for the frames an incremental elastic-plastic constitutive relation was used. The elastic constants were: Young's modulus  $E=210\text{GPa}$  and Poisson's ratio  $\nu=0.3$ , for the steel and  $E=70\text{GPa}$  for the Aluminum. The plastic range was governed by a Von-Mises yield criterion, assuming a variation of the yield strength with the strain-rate as given by eq.(1) and eq.(2) for steel and Aluminum, respectively. The value  $Y_0$  of the static yield strength was measured in quasi-static uniaxial stress tests. For the steel cylinder  $Y_0=0.40$  GPa, for the steel frame  $Y_0=0.59\text{GPa}$  and for Aluminum cylinder  $Y_0=0.32\text{GPa}$ .

#### 4. Results

##### 4.1 Water-Filled Cylinders

Two mild steel cylinders were tested, and one Aluminum cylinder. One of the steel cylinders, and the Aluminum cylinder had uniform thickness in the cylindrical section. The other steel cylinder had a variable thickness, as shown in fig. 1. The computational mesh is shown in fig. 3 for the initial time and two selected times during the motion. The final deflections for the three cases are shown in fig. 4, together with the best code predictions. For the steel cylinders, the best fit was obtained with the following parameters of eq. (1).

$$Y_0 = 0.40\text{GPa} \quad , \quad n = 5 \quad , \quad d_0 = 60/\text{S}$$

Note that the value of  $n$  is identical with the one recommended by Bodner and Symonds<sup>[1]</sup>, but that  $d_0$  is slightly larger than their recommended value of 40/S. The value of  $d$  changes threefold, approximately, for the strain-rate range of 0-1000/S in this problem.

For the Aluminum, the strain-rate sensitivity is expected to be much less pronounced. In fact, our recommended value for  $b$  in eq.(2) is identical with the one given in (2),  $b=0.15/\text{S}$ .  $Y$  changes by about 40% for the corresponding variation of strain-rate in the problem.

##### 4.2 Frames

The steel frame was deformed well into the plastic range, with a peak strain of 3.5% and a peak strain-rate of 2000/S. At this level of strain-rates we anticipated a distinct strain-rate dependence. However, the best fit to the data was obtained with a constant value of the yield stress,  $Y=Y_0 = 0.59\text{GPa}$ . (Fig. 2c). Further investigation are required to clarify this result.

## 5. Conclusions

The proposed procedure for determining the viscoplastic behavior of metals is appropriate for obtaining engineering approximation type information. It should be regarded as an economical substitute for a more thorough investigation when the mechanical properties are needed only for a gross vulnerability assessment studies.

## 6. References

- / 1 / Bodner, S.R. and Symonds, P.S.: Experiments on Viscoplastic Response of Circular Plates to Impulsive Loading:, J. Mech. Phys. Solids, Vol. 27 pp 91-113 (1979).
- / 2 / Hoge, K.G.: "Influence of Strain-Rate on Mechanical Properties of 6061-T6 Aluminum under Uniaxial and Biaxial States of Stress: Exp. Mech. pp. 204-211, (Apr. 1966).
- / 3 / Kivity, Y. and Tzur, D.: "Study of Projectile Formation in Lined Shallow Cavity Charges". Proceedings of the 4th international symposium on Ballistics, Monterey, California. 17-19 Oct. 1978.
- / 4 / Hermann, W.: "Analysis of Primary Containment Transients: Review of Phase 3 Calculations" Sandia Report SAND 82-1363 (March 1982).
- / 5 / Hancock, S.L.: Physics International Company, Technical memo TCAM 73-8 (1973).
- / 6 / Seeger, R.J. and Plachek, H.: "On Shock-Wave Phenomena: Waterlike Substances", J. App. Physics 22, 5, pp. 640-654 (1951).

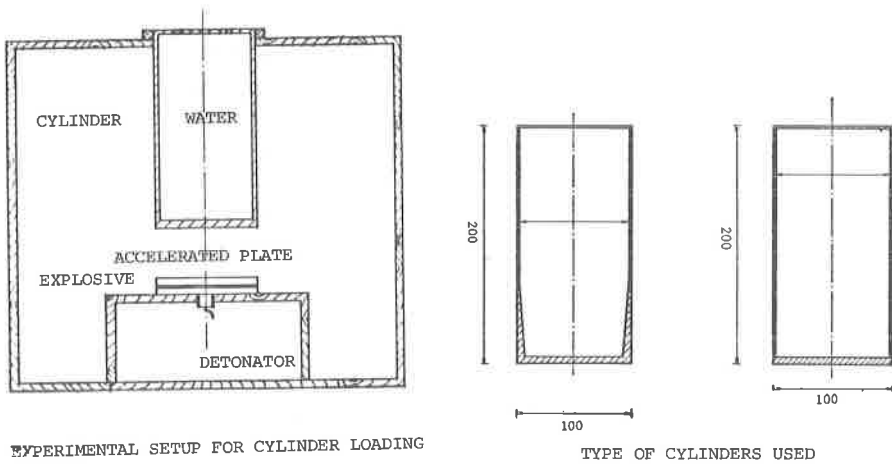


FIG. NO. 1: EXPERIMENTAL SETUP FOR IMPACT OF WATER  
FILLED CYLINDERS.

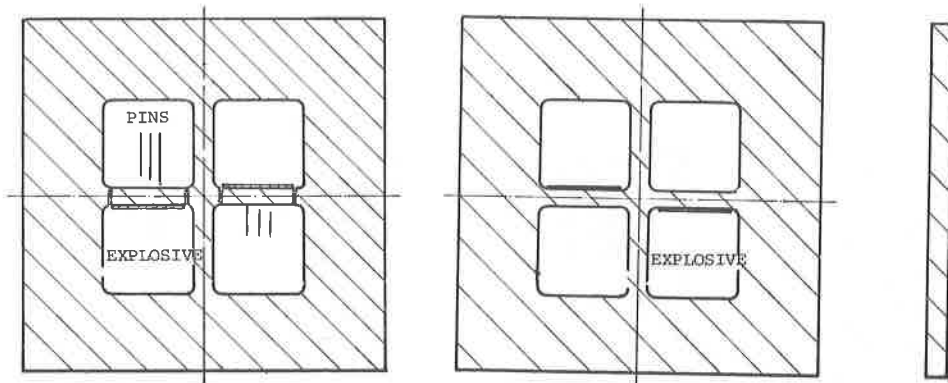


FIG. 2b: IMPULSE LOADING TRANSFER MEASUREMENTS. FIG. 2a: EXPERIMENTAL SETUP.

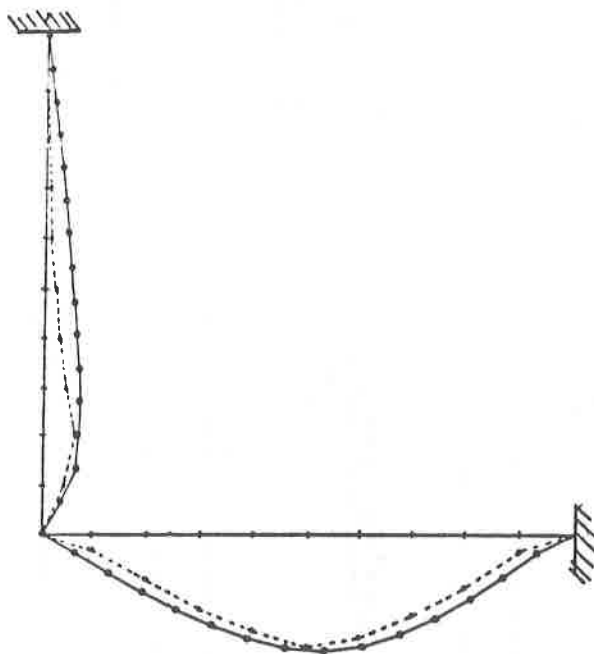
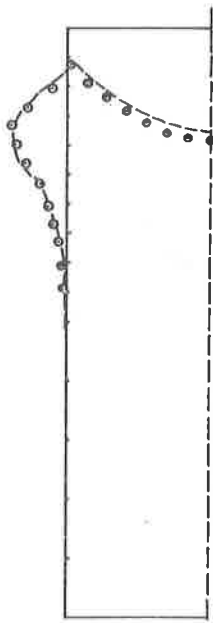
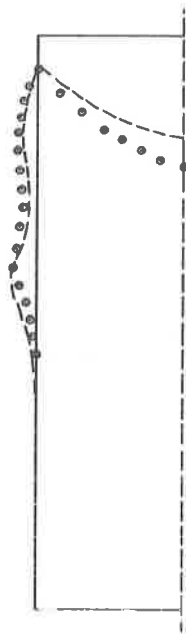


FIG. 2c: DEFORMATION IN FRAME LOADING .  
 \_\_\_\_\_ COMP.      - - - - EXPERIMENTAL.

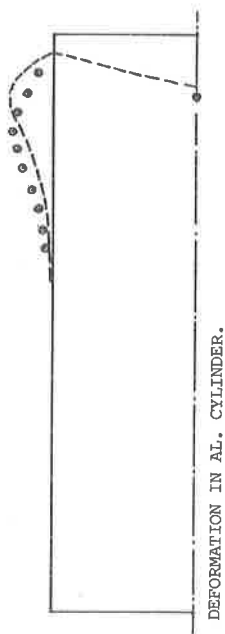
FIG. NO. 2: SETUP FOR FRAME LOADING & EXPERIMENTAL RESULTS.



DEFORMATION IN CONSTANT WALL THICKNESS STEEL CYLINDER.



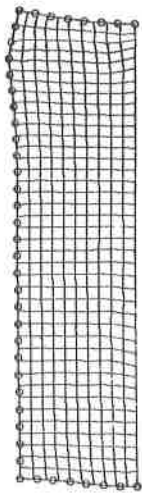
DEFORMATION IN TAPERED WALL THICKNESS STEEL CYLINDER.



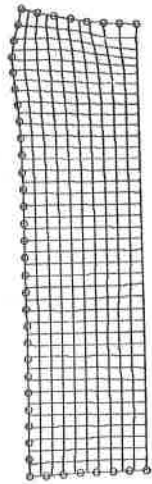
DEFORMATION IN AL. CYLINDER.

---- EXP.      COMP.

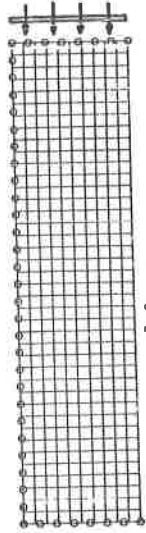
FIG. NO. 4: FINAL DEFLECTION OF CYLINDERS



$\tau = 420 \mu s$



$\tau = 140 \mu s$



$\tau = 0$

FIG. NO. 3: COMPUTATIONAL MESH AT SELECTED TIMES